Pressure Drop Analysis of Square and Hexagonal Cells and its Effects on the Performance of Catalytic Converters

Shahrin Hisham Amirnordin, Suzairin Md Seri, Wan Saiful-Islam Wan Salim, Hamimah Abd Rahman, and Khalid Hasnan

***Abstract*— Stringent emission regulations around the world necessitate the use of high-efficiency catalytic converters in vehicle exhaust systems. Therefore, determining the optimum geometry of the honeycomb monolith structure is necessary. This structure requires a high surface area for treating gases while maintaining a low pressure drop in the engine. In the present paper, an adapted sub-grid scale modeling is used to predict the pressure loss of square- and hexagonal-cell-shaped honeycomb monoliths. This sub-grid scale modeling represents the actual variations in the pressure drop between the inlet and outlet for various combinations of wall thickness and cell density. A comparison is made between the experimental and numerical results established in literature. The present approach is found to provide better and more comprehensive results than the single channel technique.**

***Index Terms*— Catalytic converter, honeycomb monolith, pressure loss, sub-grid scale modeling.**

I. Introduction

Air pollution and global warming are major issues nowadays. Hence, emission regulations introduced around the world are continually becoming stricter every year. The enforcement of these regulations has led to the compulsory utilization of catalytic converters for treating the exhaust gas emissions of vehicles.

The installation of a catalytic converter in an exhaust system has attracted numerous research. The catalyst surface needs to have a sufficient area for treating the gases to meet the emission limits. However, this procedure increases the pressure drop, resulting in engine power losses and fuel wastage. Indeed, an increased pressure drop is a very important challenge to overcome. Typically, an engine will lose about 300 W of power per 1000 Pa of pressure loss [1]. As a result, a trade-off between the pressure loss and total surface area has become the main concern in determining the appropriate geometry of catalytic converters.

The pressure drop in catalytic converters is associated with two major components: substrate and flow distribution devices (manifold, inlet and outlet pipe, as well as inlet and outlet diffuser) [2]. The substrate makes the largest contribution of the exhaust backpressure. Substrates used to be in pellet forms using spherical particulate γ-Al_2O_3 particles before being replaced with the honeycomb monolith structure. This structure has been proven more advantageous in terms of ensuring a lower pressure drop by having a high open frontal area (*OFA*; about 70%) and parallel channels [3]. The honeycomb monolith is also available in different cell densities and shapes offering potential flexibility. However, the geometries have to be optimized to meet the demands of the automotive industry.

Some previous studies [4][5] have investigated the effects of cell density and wall thickness on the performance of a catalytic converter. Basically, these studies described the number of cells per square inch (cpsi) or square centimeter (cpsc). A high cell density was found to yield a large surface area, but corresponded to a higher pressure drop. Rising manufacturing costs are also compromising mechanical durability [5]. Moreover, an increase in cell density is accompanied by a reduction in wall thickness to compensate for the increase in backpressure.

The substrate length, cross-sectional area, and cell shape are also important parameters that have been investigated by many researchers. Day [6] and Miyairi *et al.* [7] have identified the importance of cell shape in the overall performance of a catalytic converter. Pressure drop, heat, and mass transfer characteristics have been calculated in relation to different cell shapes. Nevertheless, the evaluation of the substrates in [6] and [7] does not quantify any specific criterion. Each substrate evaluated in [7] possessed different cell shapes, lengths, cell densities, and wall thicknesses. Comparisons may be further enhanced by implementing performance evaluation criteria (PEC).

Researchers have employed PEC to appropriately compare different cell shapes. Tanaka *et al.* [8] concluded via emission analyses that a square cell is better than a hexagonal one. However, the pressure drop of a hexagonal cell is lower due to its larger *OFA* and hydraulic diameter (D_h). On the other hand, when the geometrical surface areas (*GSA*) are identical, a square cell is slightly better than a hexagonal one in terms of emission levels. Andreassi *et al.* [5] conducted studies using fixed cell densities and hydraulic diameters. At a constant cell density of 300 cpsi, a square cell is more superior in terms of pressure loss. The superiority trend is square > hexagonal > sinusoidal > triangular. At a constant hydraulic diameter of 1.26 mm, the trend is triangular > sinusoidal > square > hexagonal. The backpressure, Nusselt number, Sherwood number, and pollutant mass fraction were also evaluated, but the focus was on a single cell density using single channel three-dimensional (3D) analyses. Becker *et al.* [10] included the substrate *GSA* and *OFA* in

Manuscript received June 6, 2011. The authors would like to thank the Ministry of Higher Education, Malaysia for supporting the present research under the Fundamental Research Grant Scheme (FRGS) VOT 0360.

Shahrin Hisham Amirnordin, Suzairin Md Seri, Wan Saiful-Islam Wan Salim, Hamimah Abd Rahman, and Khalid Hasnan are with the Automotive Research Group (ARG), Faculty of Mechanical and Manufacturing Engineering, Universiti Tun Hussein Onn Malaysia (UTHM), 86400 Parit Raja, Batu Pahat, Johor, Malaysia (e-mail: shahrin@ uthm.edu.my).

their study on the circular shape. The cell geometry closest to a circle provided the best conversion efficiency, in contrast with the results obtained by Andreassi *et al*. [5]. Different cell shapes may exhibit different trends toward different cell densities and hydraulic diameters, as predicted by calculations.

Other studies have indicated that the abovementioned parameters cannot be used to accurately characterize substrates with different sizes due to nonlinear relationships among the geometrical parameters. Shah and Sekulic [9] used PEC to assess the performance merits of enhanced heat transfer surfaces relative to plain surfaces in a single-phase flow. The PEC were established by selecting one of the operating variables as a performance objective to design constraints on the remaining variables. The variables considered were geometry (number of tubes and length), flow rate, fluid pumping power, heat transfer rate, and fluid inlet temperature difference. Three major PEC were developed, namely, fixed geometry, fixed flow area, and variable geometry. Using a heat exchanger application, the designers managed to determine the criteria and directly compare the performance without requiring an evaluation of the fluid properties. These properties dropped out during the performance ratio computation.

Inlet and outlet effects also contribute to the overall pressure drop. Entrance effects are due to the boundary layer growth, flow maldistribution, and sudden contraction when flow enters the monolith. A deceleration effect at the channel outlet may influence the pressure loss in that region. Therefore, a fully developed laminar flow profile would arise after a certain distance in the channel [11].

Many models have been proposed to predict the pressure loss of channel substrates with various cell shapes. The most common model is the classic Hagen–Poiseuille for a fully developed laminar flow through a circular duct [12]. Models for a square duct [12] and Luoma's expression [13] have also been obtained. Based on a comparison between the measured and model-predicted data, several conclusions have been drawn. None of these models is able to capture the exact behavior of pressure losses [11]. The equation for a square duct is accurate for calculating the static pressure at the exit of a monolith. Nevertheless, the flow profile of a monolith is different from the accepted laminar profile, which is possibly caused by the high surface roughness of the channel [11].

An empirical model has also been developed by Ekstrom and Andersson [14] to predict the pressure drop suitable for one-dimensional (1D) and 3D simulations. Only one channel was modeled. The Hagen–Poiseuille equation was used to describe the pressure drop of the laminar flow in a channel. However, literature values can be found for most of the simple shapes. For more complicated shapes, the computational fluid dynamics (CFD) simulation of a single channel can give a constant value. Experimental determinations can also be accomplished by measuring the pressure drop difference between substrates of different lengths

In a substrate, typical honeycomb channels have a hydraulic diameter-to-length ratio of 1:100. In performing calculations, if each channel is represented by a 10 × 10 × 100 cell, modeling all the channels produces millions of cells. The computations are thus tremendous and costly. Indeed, the modeling of a honeycomb monolith is rather complicated given its massive number of channels [16].

Since a honeycomb material is a unitary structure with uniform-sized and parallel channels, it is available in various channel shapes and dimensions. The shapes include hexagonal, square, sinusoidal, triangular, and circular. A macroscopic modeling of catalytic activities may be limited to a single channel of the monolith substrate. The modeling is validated by considering that the velocity profile is uniform at the inlet face of the monolith sample, assuming that flow maldistribution does not occur when the exhaust gas enters a substrate from the diffuser. Individual channels are separated from each other in terms of mass transfer, thereby providing information on the pressure loss, heat and mass transfer, as well as chemical behavior of the catalyst [16]. The single channel method of analysis has been employed by many previous researchers [4][5][7][11][14]. Fig. 1 displays the single channel modeling of a circular substrate with a square cell shape [7].

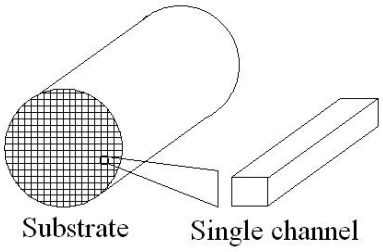

Fig. 1. Single channel modeling [7].

The increasing needs in the design and optimization of full-scale catalytic converters require further improvements in modeling techniques. A sub-grid scale modeling (Fig. 2) has been used to predict the temperature and concentration of catalytic combustion in a full-scale catalytic converter [15]. The simulation has provided certain pressure drop values from the beginning of the monolith until its end. This technique is primarily focused on heterogeneous chemical reactions, in which the prediction of temperature and concentrations within an entire catalytic converter is obtained based on a complex combination of the properties of the gas and solid parts. Such effects cannot be predicted by the single channel method. Moreover, sub-grid scale modeling has a better accuracy than the single channel method [16].

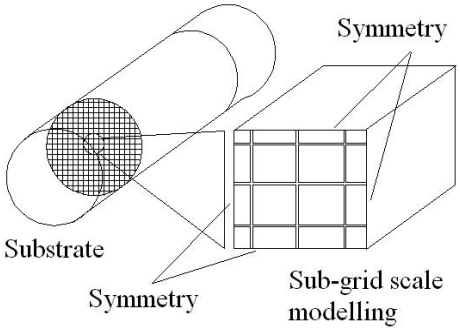

Fig. 2. Sub-grid scale modeling [15].

The present paper proposes an adapted sub-grid scale modeling to predict the pressure drop of square- and hexagonal-cell-shaped honeycomb monolith structures in an exhaust after treatment. The proposed method offers a closer approximation of the pressure loss compared with other established techniques. An additional advantage is the need for fewer elements, which reduces the computing cost. Using this model, the performances of both shapes using the PEC method are compared. The main criteria are the pressure drop and specific surface area.

Section II of the present paper describes the computational domain, geometries, meshing, boundary conditions, as well as validation and PEC methods. Section III discusses the results of the CFD calculation, including a grid independence study and model validation. This section also examines the PEC and parameters influencing the substrate performance. Section IV is the Conclusion.

II. Methodology

A. Computational Domain

Two types of honeycomb monolith structures were employed in the current study. One is square-shaped with 600 cpsi and a thickness of 4.5 mil (0.114 mm). The other is hexagonal with 400 cpsi and 3.5 mil (0.089 mm). The domain was built using the approach adapted from a sub-grid scale modeling [15], which is shown in Fig. 3 for a square and in Fig. 4 for a hexagon. Instead of considering only a single channel [7], four channels for the square and seven channels for the hexagon were utilized. The inlet and outlet lengths of these channels were simultaneously taken into account. The geometrical differences in the domain setup was compared with the single channel method, and tabulated in Tables I and II.

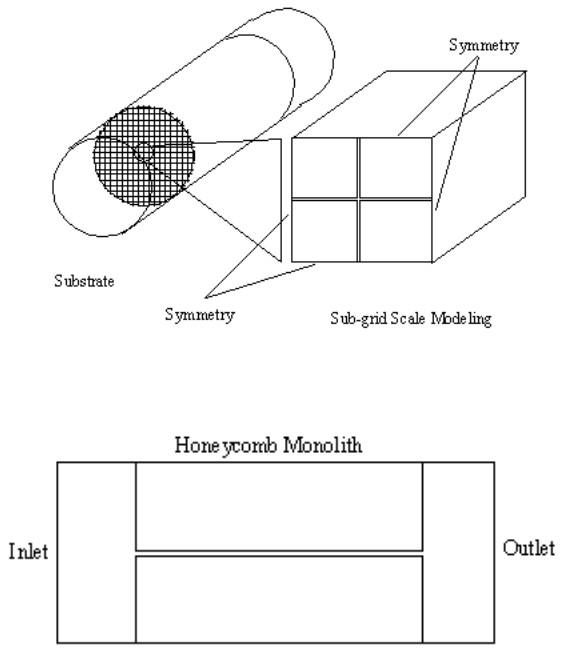

Fig. 3. Adapted sub-grid scale modeling applied on a square cell honeycomb monolith.

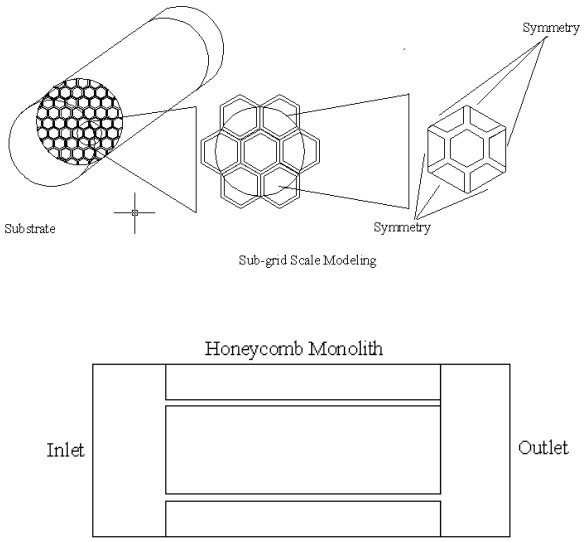

Fig. 4. Adapted sub-grid scale modeling applied on a hexagonal cell honeycomb monolith.

TABLE I. Geometries in the Single Channel [7] and Sub-grid Scale Modeling Methods

Parameters	Single channel	Sub-grid scale modeling
	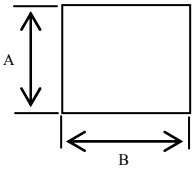	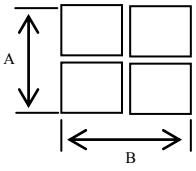
Cell shape	Square	Square
A (mm)	0.950	1.064
B (mm)	0.950	1.064
Cell length (mm)	118	118
Cell density (cpsi)	600	600
Wall thickness (mm)	0.114	0.114

TABLE II. Geometries in the Single Channel [7] and Sub-Grid Scale Modeling Methods

Parameters	Single channel	Sub-grid scale modeling
	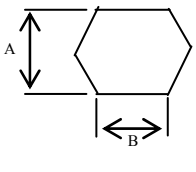	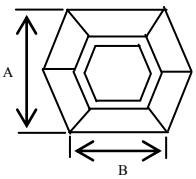
Cell shape	Hexagon	Hexagon
A (mm)	1.000	1.328
B (mm)	0.575	1.575
Cell length (mm)	69.8	69.8
Cell density (cpsi)	400	400
Wall thickness (mm)	0.089	0.089

Fig. 5 shows the actual domain with a solid T shape representing the wall thickness of the square cell honeycomb structure. An unstructured Tri-mesh (0.2 mm spacing) with 121 718 elements is depicted in Fig. 6. Fig. 7 represents the hexagonal cell domain. Fig. 8 shows the unstructured Tri-mesh with 0.34 mm spacing and 76 462 elements.

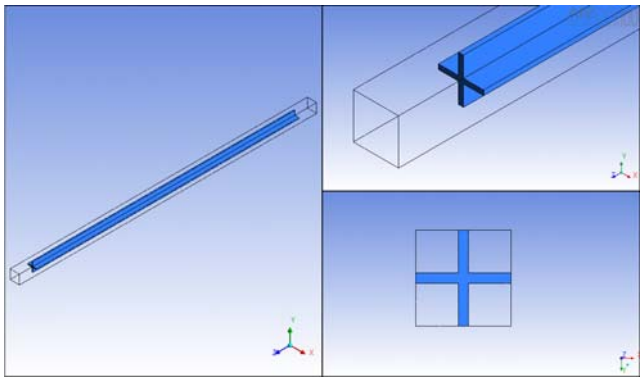

Fig. 5. Computational domain of a square cell

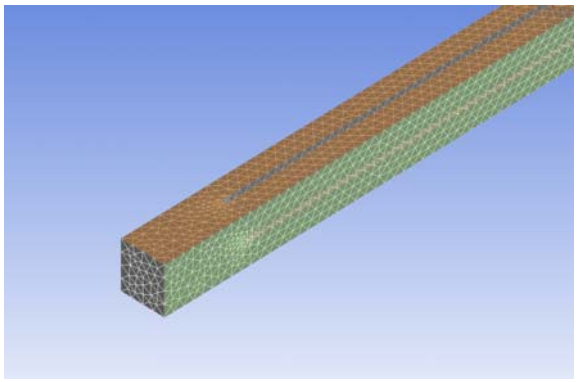

Fig. 6. Meshing of a square cell.

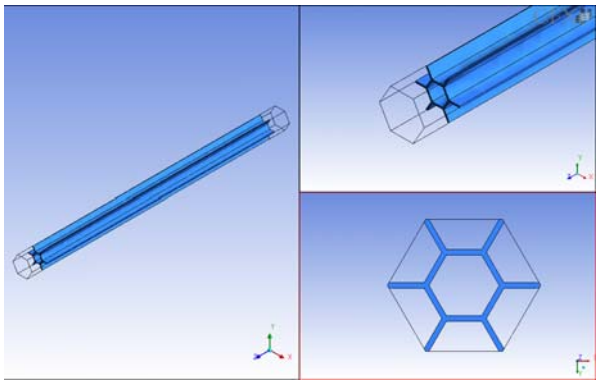

Fig. 7. Computational domain of a hexagonal cell.

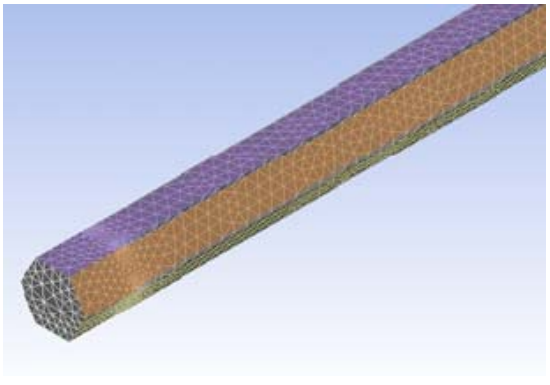

Fig. 8. Meshing of a hexagonal cell.

B. Boundary Conditions

An inlet was defined as the flow regime in the subsonic with an assumed uniform velocity of 5 m/s and an air inlet temperature of 20 °C (293 K). The air inlet temperature was selected based on the experimental and numerical conditions reported by Miyairi *et al.* [7]. As the simulation proceeded, the velocity was changed to 10, 15, and 20 m/s. The pressure outlet was set at atmospheric pressure. The wall was defined as a no slip condition at the fixed temperature of 100 °C (373 K).

The fluid properties of air used in the proposed model is given in Table III. A 3D steady-state incompressible solution of the Navier–Stokes equation was performed using the CFD software ANSYS CFX. The Navier–Stokes equations involved are the continuity and momentum equations [17], as shown in Eqs. (1) and (2), respectively.

$$\frac{\partial \rho}{\partial t} + \nabla \bullet (\rho U) = 0 \tag{1}$$

$$\frac{\partial \rho U}{\partial t} + \nabla \bullet (\rho U \otimes U) = \nabla \bullet (-p\delta + \mu(\nabla U + (\nabla U)^T)) + S_M \tag{2}$$

During the solver definition, an upwind advection scheme was used, and the convergence criteria indicated the residual type as root-mean-square (RMS). The residual target was set at 1×10^{-5}.

TABLE III: AIR PROPERTIES AT 20°C AND 1 ATMOSPHERE IN BOUNDARY CONDITIONS

Thermodynamic properties (unit)	Properties
Molar mass (kg/mol)	28.96
Density (kg/m^3)	1.205
Specific heat capacity (J/kg·K)	1005
Dynamic viscosity (kg/m·s)	18.207×10^{-6}
Thermal conductivity (W/m·K)	0.0257

C. Validation

A pressure drop calculation was performed on both honeycomb structures using the cell densities, wall thicknesses, and lengths in Tables I and II. At 5 m/s inlet velocity, the calculated results were compared with the experimental data in [7]. The difference was calculated using root-square (RS) and RMS, as respectively shown in Eqs. (3) and (4). The differences were tabulated in percentage. The same steps were applied for 10, 15, and 20 m/s inlet velocity.

$$RS = \sqrt{\left(\frac{X_{sim} - X_{\exp}}{X_{\exp}}\right)^2} \ \%, \tag{3}$$

where X_{sim} is the calculated data and X_{exp} is the experimental data.

$$RMS = \frac{1}{n}\sum_{i=1}^{i=n} RS_i \ \%, \tag{4}$$

where n is the number of data.

D. Performance Evaluation Criteria

The pressure loss of substrates varies due to their cell shapes, hydraulic diameters, lengths, cell densities, and wall thicknesses. Comparing substrate performances for certain cell shapes becomes inaccurate if the channel geometries are different. In the present study, comparisons are made using constant hydraulic diameters, cross-section areas, cell densities, and wall thicknesses. The substrate length was set at 152.4 mm (6 in), which is typical for 1500 cm^3 substrate volume applied on commercial catalytic converters. Using this criteria, the actual influence of hexagonal and square cell shapes can be reliably compared [5].

III. Results and Discussion

A. Grid Independence and Model Validation

Grid sensitivity tests were conducted using the same geometries in the experiment conducted by Miyairi *et al.* [7]. Figs. 9 and 10 illustrate the calculated pressure drop of square and hexagonal cells at different velocities and mesh densities. The small deviations in the pressure drop values of both shapes compared with the experimental values indicated the reliability of the meshing scheme for further use.

Fig. 9 shows the calculation results. The grid independence of the square cell was between 121 718 and 150 744, with the RMS differences ranging between 1.14% and 5.15%. The RMS difference for each set of data at each particular velocity exhibited the consistency between the computed and experimental pressure loss values. The preferred mesh density was selected based on the best fit between the predicted and experimental pressure drop data. Consequently, the lowest mean difference chosen was 5.14%, representing the mesh density of 121 718. This meshing scheme was selected for further use in the simulation for the square-shaped cell.

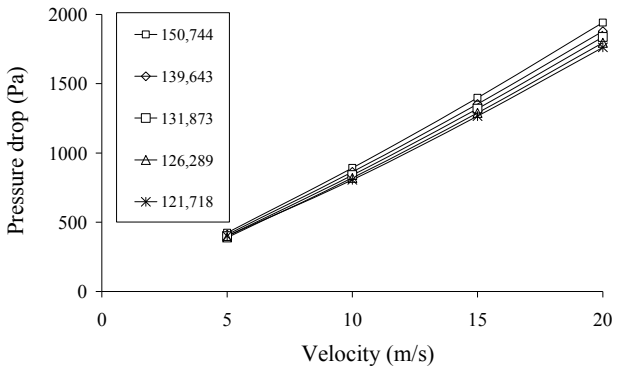

Fig. 9. Grid independence study for a square cell.

Fig. 10 shows that the mesh densities of the hexagonal structure ranged from 74,831 to 82,269, with the RMS deviations ranging from 4.04% to 6.78%. The best fit of the mesh densities was obtained with 76 462 elements and yielded the lowest RMS difference of 4.04%.

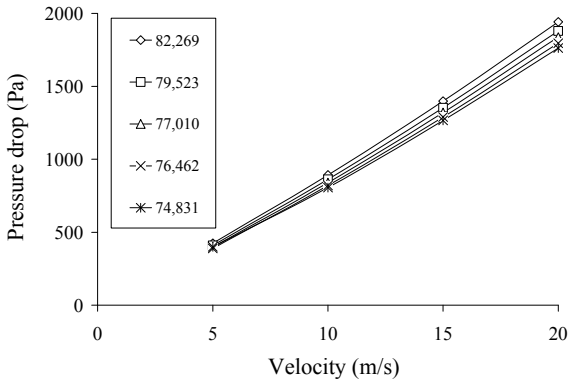

Fig. 10. Grid independence study for a hexagonal cell.

The present work was validated by comparing the simulation results from the preferred meshing to the experimental data and numerical works conducted by Miyairi *et al.* [7]. Table IV shows that the mean RMS difference of the present simulated results was 5.14% for the square cell. A previous numerical work [7] exhibited a higher deviation, with a mean RMS difference of 14.51%. Table V shows that the RMS difference in the present work was 4.05% for the hexagonal cell, which is better than the RMS difference of 9.35% in [7].

TABLE IV: Validaton for Square Cell Shape

	Miyairi *et al.* [7]			Present work	
Air velocity (m/s)	*Experiment Pressure drop (Pa)*	*Simulation Pressure drop (Pa)*	*RS diff. (%)*	*Computed Pressure drop (Pa)*	*RS diff. (%)*
5	417	476	14.16	400	4.00
10	857	987	15.10	806	5.97
15	1339	1527	14.00	1266	5.47
20	1857	2132	14.78	1762	5.12
		RMS diff. (%)	14.51	RMS diff. (%)	5.14

TABLE V: Validaton for Hexagonal Cell Shape

	Miyairi et al. [7]			Present work	
Air velocity (m/s)	*Experiment Pressure drop (Pa)*	*Simulation Pressure drop (Pa)*	*RS diff. (%)*	*Computed Pressure drop (Pa)*	*RS diff. (%)*
5	152	153	0.59	142	6.45
10	318	364	14.33	318	0.14
15	512	576	12.42	533	4.12
20	747	822	10.06	788	5.49
		RMS diff. (%)	9.35	RMS diff. (%)	4.05

The present method of prediction exhibited a higher accuracy of up to 5% deviation from the actual experiment. A parity chart is plotted in Fig. 11 showing that the present numerical work well agreed with the experimental data.

Fig. 12 compares all models (including Ekstrom and Andersson [14]) and the established Darcy equation [9]. The deviations from these two models were higher at 19.41% and 22.73%, respectively, compared with the experiment. Similar trends observed in Fig. 13 represent results on hexagonal cell.

Evidently, the present numerical approach is advantageous in predicting the pressure drop across square and hexagonal

cell channels. Sub-grid scale modeling yields better results compared with the single channel approach and other available models (Fig. 12 and 13). Its advantages include a lower computational cost (lower number of cells and computing time) and better accuracy (lower difference compared with the experimental pressure drop). Only ≤150 000 elements are employed for the square cell, compared with 300 000 to 500 000 elements used in the single channel method.

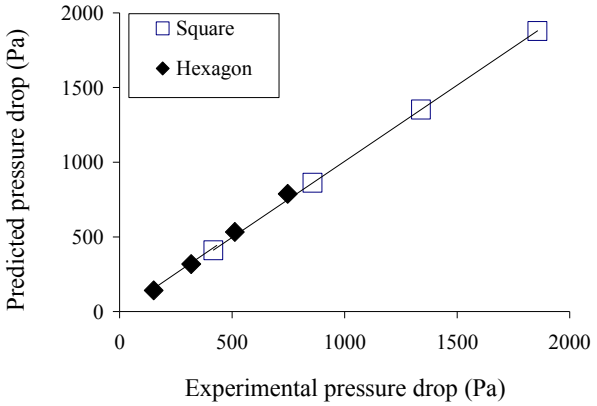

Fig. 11. Parity chart of the correlation between simulated and experimental pressure drop data.

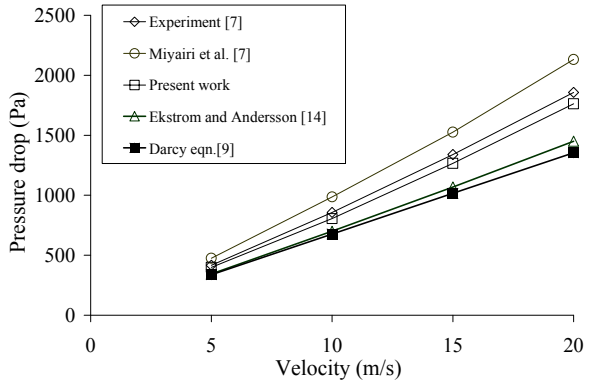

Fig. 12. Comparison of pressure drop data obtained from different techniques for a square cell.

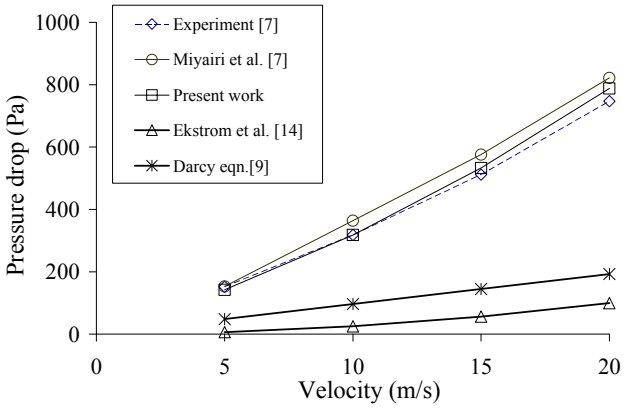

Fig. 13. Comparison of pressure drop data obtained from different techniques for a hexagonal cell.

Further comparisons of the square and hexagon cell shapes were performed using the criteria of hydraulic diameter, cross-sectional area, and cell density. The friction factor and specific surface area were used as the indices for measuring performance.

B. PEC for square and hexagonal cell shapes

The performance of a catalytic converter is mainly influenced by the substrate. The present study focused on minimizing the pressure loss due to the substrate while providing sufficient a surface area for chemical reactions to occur. Pressure loss is one of the most important parameters in gauging a catalytic converter performance. Experimental pressure loss data can be used for the design and analysis of differently sized catalytic converters operating at different temperatures and air velocity. However, the pressure loss should be presented in a universal form such that it can be applied in other geometries and operating conditions. One approach is to present pressure loss in a non-dimensional form, such as the Darcy friction factor, *f* versus the Reynolds number *Re*. This form is used when substrate geometries (e.g., hydraulic diameter and cross-sectional area) are known [6]. Using data in non-dimensional forms could also enable the combination of variables and multiple results into a single curve or set of curves [9].

C. Constant hydraulic diameter

Firstly, the hexagonal and square shapes were evaluated at a constant hydraulic diameter of 0.923 mm and length of 152.4 mm (Table VI). The cell density, wall thickness, and cross-sectional area were calculated to keep the hydraulic diameter constant for both shapes. A 0.923 mm diameter was chosen given that the typical hydraulic diameter of channels is about 1 mm. The pressure drop for each air velocity from 5 to 35 m/s was calculated using CFD, and was then converted into *f* versus *Re* (Fig. 14). *Re* was varied with the inlet velocity, and the obtained values were similar for both shapes due to the constant hydraulic diameter.

TABLE VI. GEOMETRICAL COMPARISONS AT A CONSTANT HYDRAULIC DIAMETER (0.923 mm)

Parameters	Cell density/wall thickness (cpsi/mil)	Hydraulic diameter (mm)	Length (mm)	Cross sectional area (mm^2)	Specific surface area (mm^{-1})
Square	600/4.5	0.923	152.4	0.852	4.333
Hexagon	800/4.5	0.923	152.4	0.738	4.333

Fig. 14 depicts a similar trend of simulation results for both hexagon and square shapes. A low *Re* corresponded to a high *f*. With increased *Re*, *f* decreased toward the constant values. Re values between 1000 and 2500 produced reasonable f values. At similar Re values, the hexagon shape clearly produced a lower f than the square shape.

The mechanical and chemical performance of the substrate is depicted in Fig. 15. The values in the figure were obtained at an air velocity of 20 m/s (Re = 1222), which is the typical experimental range. The hexagon exhibited a 39% lower pressure drop than the square. The specific surface areas remained similar for both shapes due to the constant hydraulic diameter.

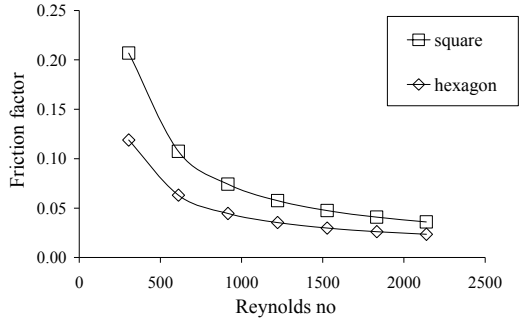

Fig. 14. Comparison of the friction factors of square and hexagonal cells at a constant hydraulic diameter.

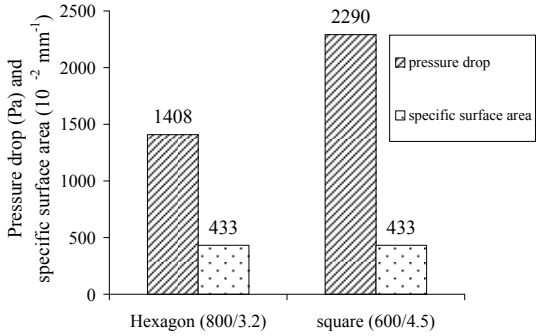

Fig. 15. Comparison of pressure drop and specific surface area at 20 m/s with hydraulic diameter = 0.923 mm and length = 152.4 mm.

D. Constant cross-sectional area

Table VII exhibits the geometrical parameters used in the simulation at a constant cross-sectional area of 0.992 mm^2 and length of 152.4 mm. The cell density, wall thickness, and hydraulic diameter were varied. *Re* was varied with the velocity and differences in the hydraulic diameters of both shapes. Fig. 16 shows that the hexagon shape had a lower *f* than the square shape at a constant cross-sectional area, which agreed with the trend at the constant hydraulic diameter. For both shapes, *f* decreased with increased *Re*.

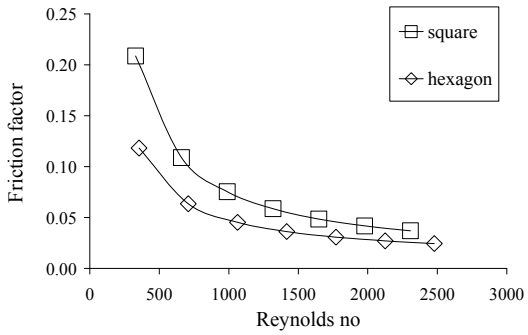

Fig. 16. Comparison of the friction factors of square and hexagonal cells at a constant cross sectional area.

Fig. 17 reveals the performance of the substrate. The pressure drop values at 20 m/s air velocity was simulated for both hexagon and square shapes. The hexagon yielded a 43% lower pressure drop than the square. However, the square possessed a 7% higher specific surface area. These results showed the superiority of the hexagon in terms of the pressure drop, and the superiority of the square in terms of the surface area.

TABLE VII: GEOMETRICAL COMPARISON AT CONSTANT CROSS SECTIONAL AREA (0.992 mm^2)

Parameters	Cell density/wall thickness (cpsi/mil)	Hydraulic diameter (mm)	Length (mm)	Cross sectional area (mm^2)	Specific surface area (mm^{-1})
Square	500/5.5	0.996	152.4	0.992	4.016
Hexagon	600/5.5	1.070	152.4	0.992	3.737

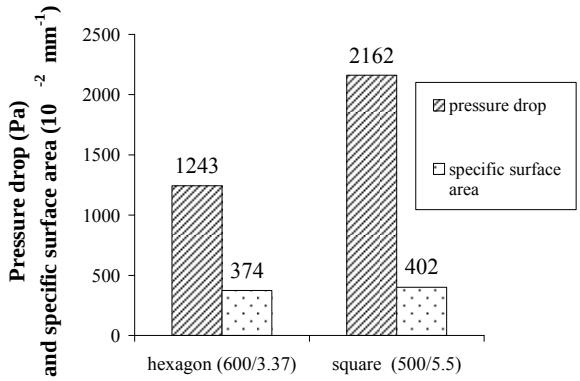

Fig. 17. Comparison of pressure drop and specific surface area at 20 m/s with cross sectional area = 0.992 mm^2 and length = 152.4 mm.

E. Constant cell density

Table VIII indicates the geometrical parameters at a constant cell density of 900 cpsi, wall thickness of 2.5 mil, and length of 152.4 mm. The hydraulic diameters and cross-sectional areas were varied to maintain the constant cell density and wall thickness. The specific surface area was calculated for both channels. *f* was calculated from the pressure drop calculation plotted against *Re*. The resulting graph is plotted in Fig. 18 and shows the similar trend already exhibited at the constant hydraulic diameter and cross-sectional area. A velocity of 5 m/s and *Re* of 290 for the hexagon yielded a high *f*. With increased *Re*, *f* decreased. This trend was also exhibited by the square shape. The performances of the substrates were compared at an air velocity of 20 m/s. The hexagon shape showed a 44 % lower pressure drop and an 11% lower specific surface area than the square shape (Fig. 19).

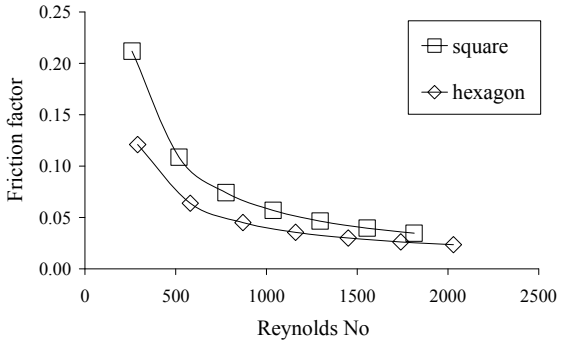

Fig. 18. Comparison of the friction factors of square and hexagonal cells at a constant cell density

.

TABLE VIII: GEOMETRICAL COMPARISON AT CONSTANT CELL DENSITY (900 cpsi)

Parameters	Cell density/wall thickness (cpsi/mil)	Hydraulic diameter (mm)	Length (mm)	Cross sectional area (mm^2)	Specific surface area (mm^{-1})
Square	900/2.5	0.783	152.4	0.613	5.11
Hexagon	900/2.5	0.876	152.4	0.665	4.56

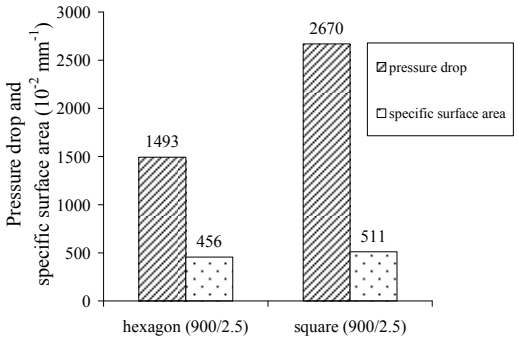

Fig. 19. Comparison of pressure drop and specific surface area at 20 m/s with cell density = 900 cpsi and length = 152.4 mm.

F. Constant wall thickness

Tables IX and X show the geometrical parameters and the simulated pressure drop for the hexagon and square shapes. The wall thickness was constant at 4.5 mil (0.114 mm), but the cell density was varied from 400 to 1200. The hydraulic diameter and cross-sectional area decreased but the length was constant (152.4 mm). The specific surface area was calculated, and the simulation results of the pressure drop at 20 m/s were obtained for each *Re*

Fig. 20 shows the plot of *f* against the cell density. *f* increased with increased cell density. The hexagon possessed a lower *f* than the square. Fig. 21 indicates that the specific surface area of the hexagon was lower than that of the square. The specific surface area increased with increased cell density, which is preferred for the chemical performance of a substrate.

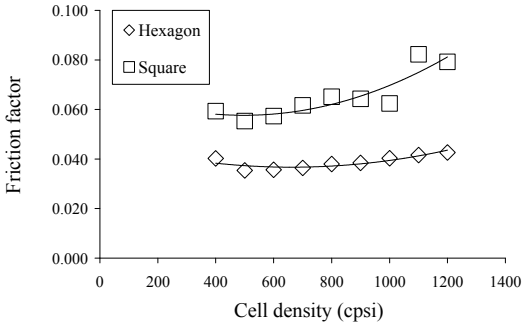

Fig. 20. Comparison of friction factor from 400 to 1200 cpsi at constant wall thickness.

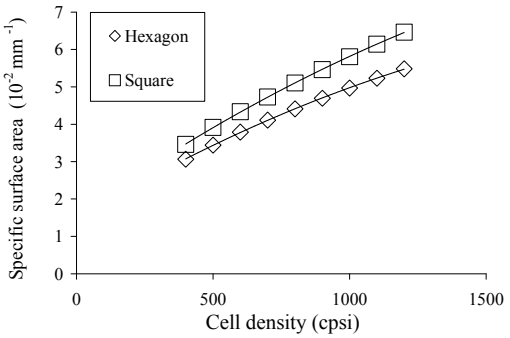

Fig. 21. Comparison of specific surface area from 400 to 1200 cpsi at constant wall thickness.

G. Various cell densities and wall thicknesses

Fig. 22 shows the plot of *f* with different cell densities and wall thicknesses against the square and hexagon cell shapes. For the hexagonal cell, *f* increased with increased cell density due to an increased pressure drop. However, the rate of increase differed for each thickness. Thicknesses of 2.5 and 3.5 mil gave low *f* values from 500 to 1200 cpsi. Thicknesses of 4.5 and 5.5 mil showed a moderate *f* values. Thicknesses of 6.5 and 7.5 mil possessed high ranges of *f*. High values of wall thicknesses (6.5 and 7.5 mil) were suitable only for substrates of low cell densities (400 to 600 cpsi). At wall thicknesses of 4.5 to 5.5 mil, only 700 to 900 cpsi cell densities gave reasonable *f* values. High cell densities (1000 to 1200 cpsi) requires thin wall thicknesses (2.5 to 3.5 mil). Therefore, appropriately selecting cell densities and wall thicknesses is critical in avoiding high *f* values obtained due to the geometry.

TABLE IX : COMPARISON OF PARAMETERS FOR A SQUARE SHAPE

No	Cell density/wall thickness (cpsi/mil)	Hydraulic diameter (mm)	Cross sectional area (mm^2)	Specific surface area (mm^{-1})	Re
1	400/4.5	1.156	1.336	3.46	1530
2	500/4.5	1.022	1.044	3.92	1352
3	600/4.5	0.923	0.851	4.34	1221
4	700/4.5	0.846	0.715	4.73	1119
5	800/4.5	0.784	0.614	5.10	1037
6	900/4.5	0.732	0.536	5.46	969
7	1000/4.5	0.689	0.475	5.81	912
8	1100/4.5	0.652	0.425	6.14	862
9	1200/4.5	0.619	0.383	6.46	819

TABLE X : COMPARISON OF PARAMETERS FOR A HEXAGON SHAPE

No	Cell density/wall thickness (cpsi/mil)	Hydraulic diameter (mm)	Cross sectional area (mm^2)	Specific surface area (mm^{-1})	Re
1	400/4.5	1.306	1.477	3.06	1729
2	500/4.5	1.162	1.169	3.44	1538
3	600/4.5	1.056	0.965	3.79	1398
4	700/4.5	0.973	0.820	4.11	1288
5	800/4.5	0.907	0.712	4.41	1200
6	900/4.5	0.852	0.628	4.70	1127
7	1000/4.5	0.805	0.561	4.97	1065
8	1100/4.5	0.765	0.507	5.23	1012
9	1200/4.5	0.730	0.461	5.48	966

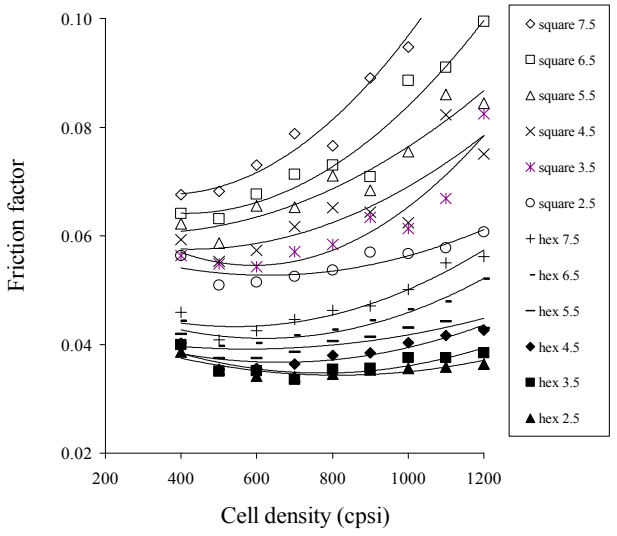

Fig. 22. Comparison of the friction factors from 400 to 1200 cpsi with wall thicknesses from 2.5 to 7.5 mil.

Generally, with increased cell density, the wall thickness needs to be thinner. This requirement can be compensated by decreasing the hydraulic diameter and cross-sectional area, which subsequently contributes to increased pressure drop. The same trend was generally observed for a square cell, as shown in Fig. 22. However, the *f* values for a square cell were in a higher range (about 0.05 to 0.11) than for the hexagon (about 0.035 to 0.055).

The hexagon possessed a lower friction factor than the square shape. Therefore, the hexagon cell was more superior in terms of mechanical performance. Fig. 23 shows the specific surface areas for both shapes. Generally, the surface area increased with increased cell density. The surface area values for the square cell were slightly higher than the hexagon cell.

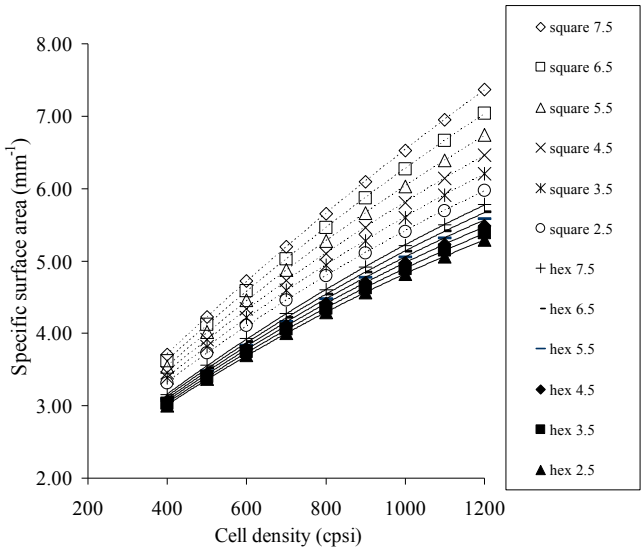

Fig. 23. Comparison of specific surface area with various cell densities (400 to 1200 cpsi) and wall thicknesses (2.5 to 7.5 mil).

Overall, the hexagon is more superior to the square in terms of mechanical performance because of the lower *f* values. However, the square shape has an advantage in terms of a higher specific surface area, which affects the chemical performance of the substrate. Using a sub-grid scale modeling, the actual influence of the cell shape on the substrate performance can be clarified.

IV. Conclusions

A sub-grid scale modeling approach yields more agreeable experimental and calculate pressure drop values than a single channel approach. This model also requires a lower computational cost because less computing time and numberof elements are required in the simulation. A sub-grid scale model approach is preferred over a single channel method because it enables the parametric studies of wall thicknesses, cell densities, hydraulic diameter, and specific surface areas.

The results also show that a hexagonal-shaped cell gives a better mechanical performance (lower pressure drop) than a square-shaped cell. On the other hand, a square-shaped cell performs better chemically (higher specific surface area) than a hexagonal-shaped cell. Overall, a hexagonal-shaped cell is more desirable than a square-shaped on because the former causes a 43% lower pressure drop.

References

[1] G.M Pannone and J.D Mueller, "A comparison of conversion efficiency and flow restriction performance of ceramic and metallic catalyst substrate," *SAE International*, 2001-01-0926, 2001.

[2] M. Lashmikantha and M. Keck,"Optimization of exhaust systems," *SAE Internationa*l, 2002-01-0059, 2002.

[3] R.A. Searles, "Contribution of automotive catalytic converters," in *Material aspects in automotive catalytic converters*, Hans Bode. Germany: Wiley-VCH, pp. 3-16, 2002.

[4] T.Shamim and H.Shen, "Effect of geometric parameters on the performance of automotive catalytic converters," *International Journal of Science and Technology*, 14, pp. 15-22, 2003.

[5] L. Andreassi, S. Cordiner and V. Mulone, "Cell shape influence on mass transfer and backpressure losses in an automotive catalytic converter," *SAE International*, 2004-01-1837, 2004.

[6] J.P. Day, "Substrate effects on light-off – part (ii) cell shape contributions," *SAE International*, 971024 , 1997.

[7] Y. Miyairi, T. Aoki, S. Hirose, Y. Yamamoto, M. Makino, S. Miwa, and F. Abe, "Effect of Cell Shape on Mass Transfer and Pressure Loss." *SAE International*, 2003-01-0659, 2003.

[8] M. Tanaka,. M. Ito, M. Makino and F. Abe, "Influence of cell shape between square and hexagonal cells," *SAE International*. 2003-01-0661, 2003.

[9] R.K Shah. and D.P. Sekulic, *Fundamentals of the Heat Exchanger Design*, New Jersey, USA.: John Wiley & Sons, 2003, pp. 414, 476-477.

[10] Becker, E.R., Watson, R., Brayer, M., Vogt, C. and Makino, M. (2001). "Prediction of Catalytic Performance During Light-off Phase with Different Wall Thickness, Cell Density and Cell Shape." *SAE International*. 2001-01-0930.

[11] E. Abu-Khiran, R. Douglas, and G. McCullough, "Pressure loss characteristics in catalytic converters," *SAE International*, 2003-32-0061, 2003.

[12] F.M. White, *Fluid Mechanics*, Singapore: Mc-Graw Hill, Inc. 295-334. 2003.

[13] M. Luoma, M. Harkonen, R. Lylykangas and J.Sohlo, "Optimisation of the Metallic Three-Way Catalyst Behaviour." *SAE International*. 971026. 1997.

[14] F. Ekstrom and B. Andersson,"Pressure drop of monolythic catalytic converters experiments and modeling," *SAE Internationals*, 2002-01-1010, 2002.

[15] O. Deutschmann, L. I. Maier, U. Riedel, A.H. Stroemann and R.W. Dibble, " *Catalysis Today*. 59, pp. 141-150, 2000.

[16] S. Mazumder and D. Sengupta,"Sub-grid scale modeling of heterogeneous chemical reactions and transport in full-scale catalytic converters," *Combustion and Flame*, 131, 2002.

[17] Manual of ANSYS CFX , 2005.

S.H. Amirnordin was born in Selangor, Malaysia on 4th Feb 1973. He received his B. Eng. in mechanical engineering from Universiti Sains Malaysia (USM) in 1997. He continued his masters degree at Universiti Tun Hussein Onn Malaysia and graduated in Masters in Mechanical Engineering in 2009.

After graduation in 1997, he gained his industrial experience as an engineer for 7 years at Hicom Decastings and Sharp-Roxy Electronics Corp. (M). In 2003, he joined Faculty of Mechanical and Manufacturing Engineering at Universiti Tun Hussein Onn Malaysia (UTHM). He actively involves in research and become project leader and member of six research grants. Currently, he ia a group leader of Automotive Research Group (ARG) in UTHM. His current research interest is focused on emission control in automotive and industry. He is also a member of Board of Engineers Malaysia (BEM) and Institute of Materials Malaysia (IMM).